

See discussions, stats, and author profiles for this publication at: <https://www.researchgate.net/publication/259222574>

In Situ Analysis of Biomass Pyrolysis by High Temperature Rheology in Relations with H-1 NMR

ARTICLE *in* ENERGY & FUELS · SEPTEMBER 2012

Impact Factor: 2.79 · DOI: 10.1021/ef301310x

CITATIONS

12

READS

79

7 AUTHORS, INCLUDING:



[Anthony Dufour](#)

French National Centre for Scientific Research

58 PUBLICATIONS 702 CITATIONS

[SEE PROFILE](#)



[M. Castro Diaz](#)

University of Nottingham

30 PUBLICATIONS 182 CITATIONS

[SEE PROFILE](#)



[Nicolas Brosse](#)

University of Lorraine

106 PUBLICATIONS 1,182 CITATIONS

[SEE PROFILE](#)



[Colin E. Snape](#)

University of Nottingham

426 PUBLICATIONS 7,054 CITATIONS

[SEE PROFILE](#)

In Situ Analysis of Biomass Pyrolysis by High Temperature Rheology in Relations with ^1H NMR

Anthony Dufour,^{*,†} Miguel Castro-Díaz,[‡] Philippe Marchal,[†] Nicolas Brosse,[§] Roberto Olcese,[†] Mohamed Bouroukba,[†] and Colin Snape[‡]

[†]CNRS, Lorraine University, Reactions and Processes Engineering Laboratory (LRGP), ENSIC, 1 rue Grandville, B.P.20451, 54000 Nancy Cedex, France

[‡]Nottingham Fuel and Energy Centre, School of Chemical, Environmental and Mining Engineering, Nottingham University, Nottingham NG7 2RD, United Kingdom

[§]Lorraine University, Faculté des Sciences et Techniques, LERMAB, B.P.239, 54506 Vandoeuvre les Nancy Cedex, France

ABSTRACT: The extent of softening during biomass pyrolysis is of high importance for fundamentals and reactors design but was not yet quantified *in situ*. We provide the first *in situ* rheology and ^1H NMR analysis during the pyrolysis of biomass (*Miscanthus*), microgranular cellulose, ethanol organosolv lignin, and xylan. *In situ* rheology reveals the viscoelastic behavior of the materials. The softening, resolidification (char formation), swelling, and shrinking behaviors are quantified during pyrolysis in real-time. These phenomena are discussed. The ^1H NMR analysis gives the mobility of protons developed during pyrolysis. A viscous and mobile material is formed during cellulose and xylan pyrolysis, even at a slow heating rate (5 K min^{-1}), by products at liquid phase under reaction temperatures. For lignin, a soft material and mobility are first formed by glass transition phase, then overlapped with covalent bond scission, leading to a completely mobile material. The comparison between ^1H NMR and rheology results shows that mobile liquid-like products are trapped inside elastic solid-like cavities. Strong interactions between polymers in the native biomass network are evidenced. Cellulose tends to impose its visco-elastic behaviors to the polymers network during biomass pyrolysis. Rheological signatures are also of practical interest to design feeders and reactors for polymers biosourcing, biomass gasification, or combustion.

1. INTRODUCTION

Pyrolysis is the first chemical phenomenon that occurs in all thermochemical reactors.

When a biomass particle is heated, it undergoes chemical and physical modifications that depend on the heating rate profile (or rather the external heat transfer coefficient),^{1,2} particle size,^{3,4} final temperature,⁵ pressure,⁶ etc. It is of high importance to better understand the coupled chemical and structural modifications of biomass-char particles for optimizing the design of all thermochemical reactors (pyrolysis, gasification, combustion).

Pyrolysis reactions lead to the formation of hundreds of volatile species and to char.^{7–11} Char consists of disordered aromatic sheets resembling a “crumpled paper” at the molecular scale.¹²

Numerous works have dealt with microscopic observations (optical or scanning electron microscopy (SEM) and transmission electron microscopy (TEM)) of structural change during biomass pyrolysis.^{13–23} Quantitative methods were developed for measuring char structural properties using image analysis^{19–21} combined with surface area measurement.²¹ It gave very interesting insights into the morphological changes of biomass-char particles including particles shape, size, pores, holes formation in cell walls, etc.^{19–21} It has also been shown that liquid pyrolysis products can be trapped in the pores revealing strong mass transfer limitation for the escape of pyrolysis products.^{20,24}

Magnetic resonance imaging has been used at room temperature to study combustion in burning cigarettes after

quench of cigarettes.²⁵ Imaging methods were employed to monitor substances with high molecular mobility, such as water, smoke condensate, and waxy materials, and more rigid components, such as tobacco cell wall polysaccharides and cellulose acetate fibers inside the filter. This advanced imaging method gave two-dimensional distribution of combustion and pyrolysis products deposited on the unburned portion of tobacco.²⁵

Real time imaging of biomass pyrolysis in the hot stage of a microscope also gave important new findings on the evolution of biomass tissue such as cell wall expansion, contraction, and evolution of macroporosity during pyrolysis.²⁰ To the best of our knowledge, this work is the only one dealing with *in situ* observations and liquid products formation in relation to cell wall evolution.

All previous works agreed that bubbles are formed from volatiles “pushing” a melted material.^{15,19,21} The extent of softening and bubbles depends on biomass composition and thermal conditions. Lignin and xylan would be the main source of this melted residue at low heating rate^{14–16,26} but cellulose could also form a melted residue at high heating rate.^{15,16,27–30} Moreover, the presence of minerals can affect the formation of this intermediate “liquid” phase.^{16,29,31}

It is known for at least one century that biomass forms an intermediate “liquid-like” phase or “melted residue” during

Received: August 8, 2012

Revised: September 13, 2012

Published: September 13, 2012

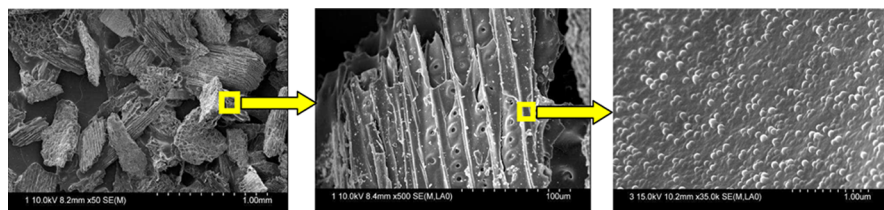


Figure 1. SEM pictures of a wood char produced under slow heating rate from mm to μm length scales.²⁴ The overall wood cell macro-structure is preserved at the 0.1 mm scale despite the important loss of cell wall material after pyrolysis.²⁰ Bubbles on the cell wall are formed by volatiles pushing a viscoelastic material at the μm length scale.¹⁵

pyrolysis,^{14,26–29,32,33} even if it has been controversial.^{30,34} Some researchers did not notice the melted residue at slow heating rate (refs in ref 30), maybe because the observation of particles was not conducted at the suitable scale needed to see the melted material.

Figure 1 was obtained from a wood char pyrolyzed under slow heating rate profile.²⁴ It shows that under these thermal conditions, the overall wood cell macrostructure is preserved at the 0.1 mm scale despite the important loss of cell wall material after pyrolysis, in agreement with ref 20. Nevertheless, there is a cell wall surface at the μm scale showing the formation of bubbles by volatiles pushing a viscoelastic material.

Despite all these extensive works on biomass particles imaging, there is still a strong lack of understanding the origin and formation conditions of this melted material. To our point of view, non-intrusive *in situ* analysis of biomass particles can give better insight into the fundamentals of pyrolysis and the intermediate “melted” material.

In-situ ^1H NMR and rheology analyses have been extensively used for studying “metaplast” formation during coal pyrolysis^{35–39} and blends.^{40–43} Gieseler plastometry (a normalized method simpler than rheology) has been also used for studying coking behavior of coal and blends.⁴⁴

To the best of our knowledge, *in situ* ^1H NMR and rheology have never been used for biomass and its polymers (cellulose, lignin, xylan).

In a first paper,³¹ the mobility developed during the pyrolysis of biomass (*Miscanthus*), cellulose, lignin, xylan, a synthetic blend of this polymer and a demineralized biomass was studied by means of ^1H NMR analysis. The effects of minerals and cellulose structure and the interactions between polymers.

In this paper, we present the results from *in situ* rheology analysis and put them in relation with the ^1H NMR data. First, ^1H NMR results for biomass, lignin, cellulose, and xylan are only briefly presented. Second, rheology results that give the evolution of the viscoelastic behaviors of material are depicted. We introduce the concept of the “rheological signature” for biomass polymers undergoing pyrolysis. Softening, swelling, shrinking, and solidification mechanisms are discussed. Finally, the rheology results are put in relation with the ^1H NMR analysis.

2. MATERIALS AND METHODS

2.1. Preparation of Samples. Cellulose (microgranular, Sigma Aldrich), xylan from birch (Sigma Aldrich), lignin extracted from *Miscanthus* by ethanol organosolv process, and *Miscanthus x giganteus* were used in this study. *Miscanthus* was harvested in North East of France, crushed, and sieved between 40 and 80 μm . The extraction procedure for lignin has been chosen to be the softest one to preserve the native form of

lignin. The detailed procedure and conditions for ethanol organosolv process can be found in refs 31 and 45.

Lignin has been extensively characterized by ^{13}C , ^{31}P NMR for quantification of functional groups and gel permeation chromatography (GPC) for molecular weight distribution. All characteristics can be found in refs 31 and 45. Elemental and ash analysis were previously given for all samples.³¹

All materials were used as powder for thermogravimetry and ^1H NMR analysis. For rheology tests, 1 g of powder were pelletized in a 25 mm die at 5 mm/min until 45 kN for *Miscanthus*, cellulose, and xylan, to form disks with a thickness of around 2 mm (INSTRON press). Lignin was pressed until 3 kN, due to a better ability to form a disk.

2.2. Thermogravimetric Analysis (TGA). TGA analysis was conducted in a TG-DSC 111 (Setaram, France) where about 2 mg of material, placed in a graphite crucible (homemade), was heated under N_2 (analytical purity) at 5 K min^{-1} (heating rate of the TGA furnace) from 20 to 500 $^\circ\text{C}$, followed by 10 min at 500 $^\circ\text{C}$. We are aware that reactions can occur at temperatures higher than 500 $^\circ\text{C}$, especially for lignin, but the aim of this work was to investigate the TG properties in the same range of temperatures as for mobile protons and viscous material development.

2.3. ^1H NMR Analysis. The fundamentals of *in situ* ^1H NMR analysis are just briefly recalled. The mobility of materials (coals, plastics, etc.) undergoing pyrolysis has been analyzed *in situ* by high temperature ^1H NMR or proton magnetic resonance thermal analysis (PMRTA) for a long time.^{35–39} The PMRTA technique measures the protons transverse relaxation signal stimulated by a solid echo pulse sequence ($90^\circ-\tau-90^\circ$). This signal is used in preference to the free induction decay, since it does not suffer from the “dead-time” loss of its initial decay.⁴⁶ The rate of decrease in the intensity of the ^1H NMR signal is determined by the strength of the magnetic couplings and the extent to which protons are static on a time scale of microseconds.⁴⁷ Protons separated by less than ~ 1 nm in rigid organic materials have strong static coupling. Their ^1H NMR signal exhibits short-lived, Gaussian-like distribution functions (relaxation time, T_2 , of 16–24 μs).⁴⁷ On the opposite, protons in mobile (“liquid-like”) molecular structures exhibit weaker static magnetic interactions. Their ^1H NMR signal decreases at a much slower rate and gives long-lived protons, Lorentzian-like distribution functions (T_2 of 100–1000 μs).⁴⁷

The Fourier-transformed time domain decays of the solid echo pulse signal were deconvoluted into Gaussian and Lorentzian distribution functions (see Figure 2) by a Matlab program. The fittings regression coefficients (R^2) are most of the time better than 0.995 and always higher than 0.99. The program enables the calculation of the fraction of mobile hydrogen or fluid phase (% H_L) from the following relation:

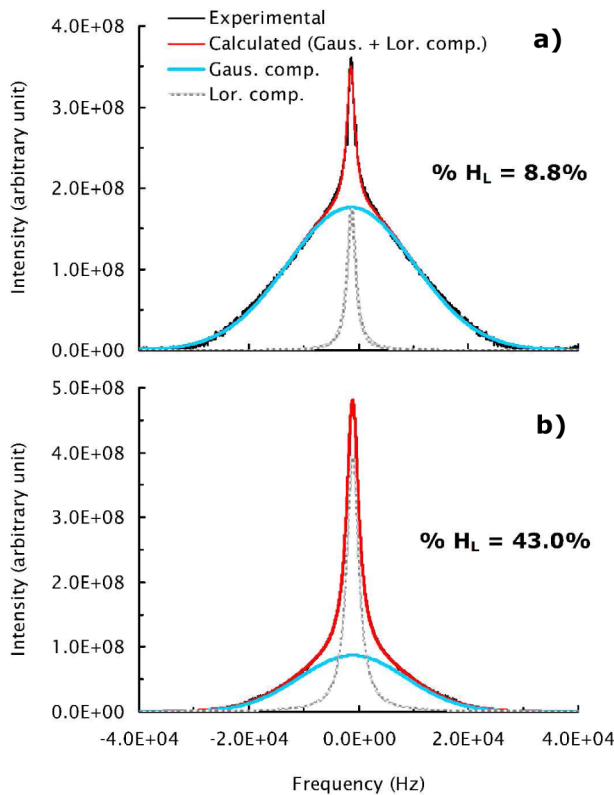


Figure 2. ^1H NMR spectra with deconvolutions into Gaussian and Lorentzian distributions and the calculated fraction of mobile hydrogen ($\% \text{ } \text{H}_L$) for Miscanthus at (a) 200 °C and (b) 300 °C heated at 5 K min $^{-1}$ in the ^1H NMR probe. When mobile protons increase from 200 to 300 °C, the signal becomes “thinner” with a higher contribution in Lorentzian function. Calculated (red) and experimental (black) curves are on top of each other.

$$\% \text{ } \text{H}_L = \frac{A_L}{A_L + A_G} \quad (1)$$

where A_L and A_G are the areas of the Lorentzian and Gaussian functions, respectively.

The relaxation times (T_2) for the protons responsible for the Lorentzian and Gaussian distribution functions were also calculated³¹ but not presented in this paper.

When mobile protons increase as a result of an increase in temperature, as for Miscanthus between 200 and 300 °C in Figure 2, the NMR peak becomes “thinner” with a higher contribution from the Lorentzian component. The peak width

of the Lorentzian distribution function is inversely proportional to the spin–spin relaxation time of the mobile phase (T_{2L}), which, in turn, is proportional to the mobility of the fluid material.

A Doty 200 MHz ^1H NMR probe was used in conjunction with a Bruker MSL300 instrument to acquire ^1H NMR spectra. A flow of 25 dm 3 min $^{-1}$ dry nitrogen was used to transfer heat to the samples and to remove the volatiles that escaped from the container. Below the sample region, a flow of 60 dm 3 min $^{-1}$ of dry air prevented the temperature rising above 50 °C to protect the electrical components. In addition, air was blown at a rate of 20 dm 3 min $^{-1}$ into the region between the top bell Dewar enclosing the sample region and the outer side of the probe. This prevented the temperature from exceeding 110 °C. The sample temperature was monitored using a thermocouple in direct contact with the sample container. The system was calibrated using compounds of known melting point (see ref 38 for more details). A pulse length of 3.50 μs was maintained throughout the test. 100 scans were accumulated using a recycle delay of 0.3 s. Approximately 50 mg of sample was handled into a boron nitride container. The samples were heated in the ^1H NMR probe from room temperature to the final temperature at approximately 5 K min $^{-1}$. Triplicate analyses were carried out with Miscanthus to verify the good reproducibility in the results. The mobility development was not affected by variations of Miscanthus particles size (40–80 and 80–200 μm) and sample weight (10, 50, and 100 mg) in the NMR probes (results not shown). The mobility development is thus not affected by heat or mass transfer effects under the range of investigated conditions.

2.4. Rheology Analysis (Mechanical Spectroscopy).

The basics of in situ rheology analysis are briefly presented. Figure 3 displays a simplified scheme of the rheometer. Measurements were performed using a Rheometrics RDA-III high-torque controlled strain rheometer. The disk of biomass was placed between two serrated plates (homemade at CNRS Nancy, in stainless steel) to reduce “slippage”.

Biomass between the plates and rheometer axe are inside a furnace flushed under N₂ (analytical purity). Plates are heated through convection of N₂, and the temperature is monitored by a thermocouple placed inside the bottom plate. The furnace can be open allowing a “quench” of the sample at a specific temperature.

Consistency between ^1H NMR and rheology results on the “melted temperature” measurement (see below) and the good heat transfer by conduction between plates and the disk (2 mm thickness) show that there are few heat transfer effects between

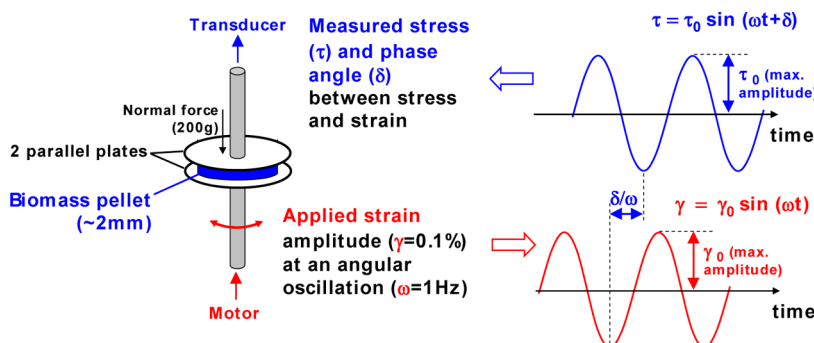


Figure 3. Simplified scheme of the rheometer with imposed (in red) and measured (in blue) parameters. Plates and biomass pellet are flushed under N₂ and placed inside a furnace controlled by a thermocouple positioned in the bottom plate through the bottom axe.

all the experimental set-ups, especially considering the slow heating rate imposed in all set-ups (5 K min^{-1}). We are aware that heat and mass transfers could be an important issue for higher external heating rates.^{1,24,34}

A very small amplitude angular oscillation was applied to the sample from the bottom plate (Figure 3).

Tests were performed with 0.1% strain amplitude (γ , amplitude of oscillation divided by disk thickness) and a frequency (ω) of 1 Hz (6.28 rad s^{-1}) following the procedure optimized in ref 48 to operate in the linear viscoelastic region of the material. The stress response (amplitude, τ_0 , and phase angle, δ) was measured on the top plate to obtain G' , G'' , and $\tan(\delta)$. These parameters are calculated and defined as follows:

$$G' = \cos(\delta) \frac{\tau_0}{\gamma} \quad (2)$$

G' (Pa) is the elastic modulus. It is proportional to the mechanical elastic energy stored and reversibly recovered.

$$G'' = \sin(\delta) \frac{\tau_0}{\gamma} \quad (3)$$

G'' (Pa) is the viscous modulus. It is proportional to the mechanical energy irreversibly lost through viscous dissipation.

$$\tan(\delta) = \frac{G''}{G'} \quad (4)$$

When $\tan(\delta) > 1$, the material exhibits mainly viscous properties; when $\tan(\delta) < 1$, it exhibits mainly elastic properties.

Throughout the test, a constant normal force of 200 g was applied to the sample from the top plate to reduce slippage. Therefore, the thickness of the sample was allowed to change. The thickness (ΔL) could be measured throughout the test and gives an indication of how much the sample is expanding/contracting.

The normal force of 200 g was automatically stopped if the elastic modulus (G') became lower than 10^5 Pa for lignin. In this case, the material becomes too soft and the auto tension condition (200 g) is stopped to avoid contact between plates, and the displacement of plate is not meaningful.

3. RESULTS AND DISCUSSION

TGA (mass loss), ^1H NMR spectroscopy (mobile protons), and rheology (viscoelastic behavior) are complementary analyses to characterize the thermal conversion of a material. The coupling of such complementary techniques is needed to better understand physical-chemical phenomena of biomass pyrolysis. ^1H NMR results are first briefly depicted. The mass losses of the samples are presented with the rheology results to help establishing relationships between the evolutions of the viscoelastic properties with mass loss. Finally, the rheology results are put in relations with the ^1H NMR data.

3.1. Evolution of Mobile Protons from in Situ ^1H NMR Analysis. The origin of mobility has been extensively discussed elsewhere.³¹ Only the main findings are recalled here.

The amount of fluid phase (% H_L) that the materials develop at their temperature of maximum fluidity decreases in the order: lignin (100% H_L) > xylan (61%) > Miscanthus (42%) > cellulose (28%).

The mobility development is shortly discussed for each individual material.

Lignin becomes completely fluid (100% H_L) at 200–225 °C and remains completely fluid up to 350 °C (Figure 4). At

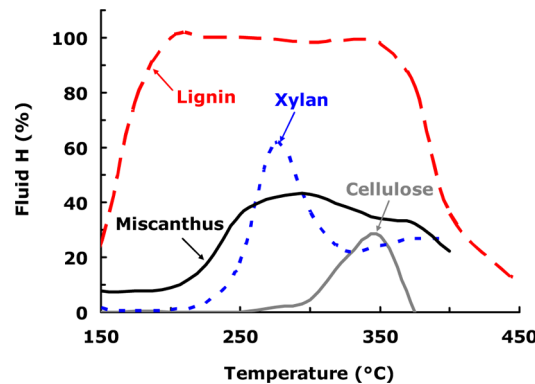


Figure 4. Fluid phase (% H_L mobile protons) development as a function of temperature. Sample heated in the ^1H NMR probe (5 K min^{-1}).

temperatures below 200 °C, the glass transition of lignin is evidenced by the increase in fluidity without any mass loss and any thermal signal (results from DSC analysis not shown). The rubbery phase mobility is then overlapped by covalent bond scission. The chemical structure of lignin is affected by the thermal treatment above 200 °C through homolytic cleavage of aryl ether linkages (mostly β -O-4 linkages).^{49–52} Small lignin fragments with a high molecular mobility are produced. With increasing temperature from 225 to 350 °C, the thermal depolymerization of lignin is associated with the well-known demethoxylation and recondensation reactions. From 350 °C, the mobile fraction decreases due to the formation of solid compounds from cross-linking and growth of aromatic domains.^{50,52,53} The decrease in the mobile H fraction evidenced from 350 °C (Figure 4) is in accordance with the solidification stage within the lignin char observed at 350–400 °C in ref 17.

Regarding cellulose, the proportion of mobile hydrogen is lower than that in lignin or xylan (Figure 4), but mobile protons from cellulose pyrolysis are evidenced for the first time even at low heating rates (5 K min^{-1}). The fluidity starts to increase slowly from 250 °C, whereas mass loss starts at 290 °C (see Figure 5) and increases sharply at 350 °C. The observed mobile phase is probably not the “active cellulose” (cellulose with a low degree of polymerization of around 200⁷). The mobile phase is probably developed by disordered carbohydrates¹¹ that can become liquid under pyrolysis conditions.^{6,20,24,28–30} Our in situ observations are consistent with proposed mechanisms that include intraparticulate liquid tar formation.^{6,24,28,54}

Xylan develops a mobile phase that increases from 200 to 275 °C (61% H_L , Figure 4). It is in agreement with microscopic observations showing that xylan shows signs of melting or softening from 200 °C.¹⁵ Contrarily to lignin, the mobile phase from xylan is developed only after the beginning of mass loss (from 200 °C). Consequently, the development of fluid material during xylan pyrolysis should not be due to a physical conversion of the native xylan but most probably from some pyrolysis products that are liquids at reaction temperature. There is still a lack of knowledge of xylan pyrolysis to discuss more in depth the origin of its fluidity.

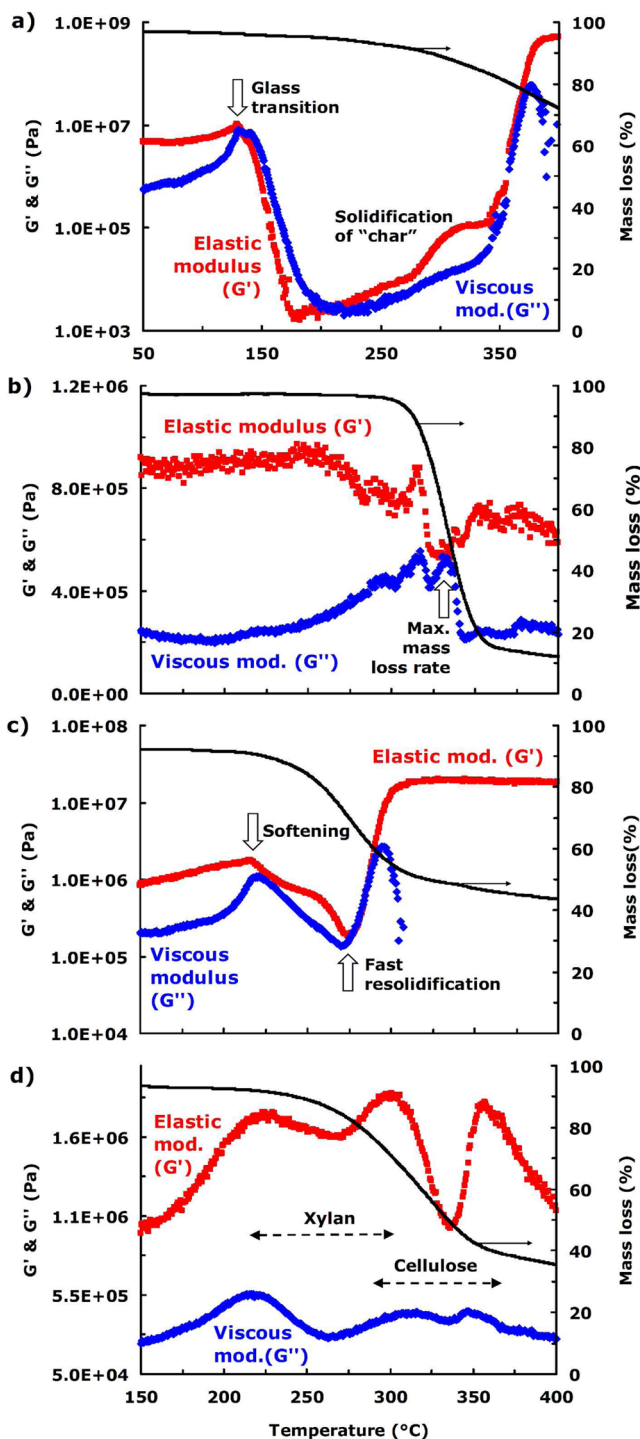


Figure 5. Evolution of elastic (G') and viscous (G'') modulus (from high temperature rheology) and mass loss (obtained by TGA) as a function of temperature (5 K min^{-1}) for (a) lignin (50–400 °C), (b) cellulose (150–400 °C), (c) xylan, (d) Miscanthus.

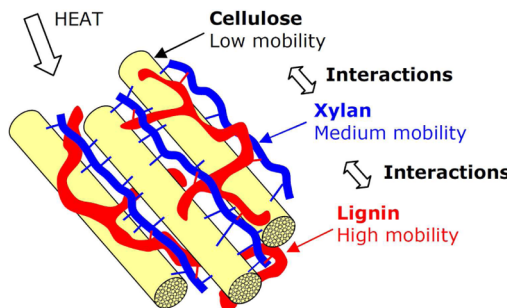
Concerning the native polymer network in Miscanthus, its mobility starts at 200 °C, but mobility starts before 150 °C for the isolated lignin (Figure 4). The ^1H NMR results are in agreement with previous SEM observations, where lignin-rich xylem elements from tobacco did not “melt” until after 300 °C, whereas isolated lignin “melted” at a lower temperature showing interactions among components in the cells wall matrix.¹⁶

Donohoe et al.⁵⁵ showed that a dilute acid pretreatment causes lignins to coalesce into larger molten bodies that migrate within and out of the cell walls of maize and can redeposit on the surface of plant cell walls. Droplets of lignin have been evidenced from 150 °C at the surface of maize cell walls. This temperature of lignin “softening” in the native cell walls is lower than in our case and ref 16, probably due to the aqueous dilute acid environment, which promotes mobility of lignin in the native network of polymers.

It is important to note that the isolated lignin has a lower molecular mass than the native one⁴⁵ that could increase its mobility at a lower temperature.

The mobility starts always at a higher temperature and to a lower extent in native networks, such as in Miscanthus, rather than in synthetic blends.³¹ It reveals strong interactions between the polymers and their pyrolysis products inside the native network that are not evidenced by the additivity law on global mass loss (in accordance with our TG results). These interactions could be explained from the structure of cell walls illustrated in Scheme 1.

Scheme 1. Simplified Scheme of the Polymers Network in the Native Biomass Cells Wall (Adapted with permission from refs 20 and 56. Copyright 2009 American Chemical Society and 2010 American Chemical Society, respectively.) and Mobility Development during Their Thermal Conversion. Cellulose “Imposes” Its Rigidity to the Polymer Network during Pyrolysis of Biomass Cell Walls



The rigidity in cell walls arises from the crystallinity of the cellulose in the microfibril phase and from cross-linking of lignins in the matrix.⁵⁷ It could explain partly why the cellulose seems to “impose” its rigidity in the native network. When fractionating the biomass polymers, lignin and xylan give rise to higher mobility after extraction because they are no longer chemically linked with cellulose (even indirectly for lignin linked to xylan, xylan directly linked to cellulose). The beginning of mobility in Miscanthus (200 °C) may be related to the beginning of xylan mass loss and/or to lignin–xylan bonds scission (ester and ether bonds).

3.2. Evolution of Viscoelastic Properties Obtained by *In Situ* Rheology Analysis. Elastic and viscous moduli for lignin (displayed between 50 and 400 °C), cellulose (150–400 °C), xylan, and Miscanthus are depicted with mass losses in Figure 5. All materials were heated from room temperature to 400 °C at 5 K min⁻¹ in the rheometer, and the moduli were measured during the pyrolysis process. Mass losses were obtained from separate experiments in TGA.

The glass transition phase of lignin is observed by rheology in agreement with the mobility development analyzed from ^1H NMR. Lignin becomes mainly viscous (viscous modulus higher

than elastic modulus) from 130 °C before any mass loss (Figure 5a). From about 140 °C, both moduli decrease, showing the formation of a soft material. Softening of lignin is due to the glass transition phase followed by bonds breaking giving lower molecular weight species. Elastic modulus reaches its minimum value ($\sim 10^3$ Pa) at 180 °C, whereas viscous modulus at 220 °C. Before 200 °C, lignin is already degraded and darkened, in agreement with small mass loss. It is a soft and mainly viscous material. This behavior is illustrated by Figure 6,

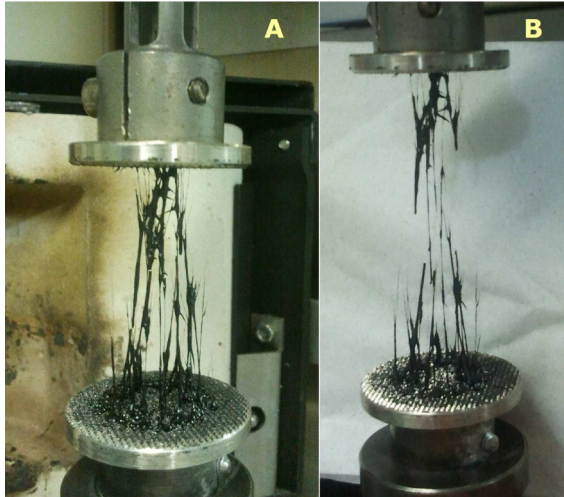


Figure 6. Photographs of rheometer plates showing degraded (darkened) lignin that form thin wires at 200 °C. (A) Furnace was quickly opened and the height between plates was quickly increased to form the thin wires when the material was still hot (<200 °C). Degraded hot lignin is a sticky, soft, and mainly viscous material like a "hot caramel". (B) After cooling of material, the height between plates was increased for a second time, showing the break of the hardened and brittle wires.

which was obtained after the quench of the sample at 200 °C by a fast opening of the rheometer furnace followed by a fast displacement of the plates. In part A of Figure 6, it can be seen that hot (<200 °C) degraded lignin forms thin wires like a hot "caramel". However, after a few seconds of cooling, these thin wires become hard and brittle, and they break due to tension strength. In part B, height between plates has been increased after cooling of the lignin-based wires showing the break of wires.

From 200 °C, the elastic modulus becomes higher than the viscous modulus (Figure 5a). The material is still soft, with low moduli, but it becomes mainly elastic. Both moduli increase from 220 °C. From 350 °C, a fast solidification of the material occurs in close agreement with the decrease in mobile protons fractions evidenced by ^1H NMR (Figure 4). Cross-linking reactions lead to the formation of a solid matrix, mainly elastic and hard: a solid "char". At 380 °C, the viscous modulus decreases and the material becomes very elastic. The macrostructure of the fluffy char¹⁷ depends on the competition between the formation of volatiles that push the viscoelastic material and cross-linking reactions that harden the structure into a mainly elastic and less deformable material. Relations between SEM observations and rheological behaviors are out of the scope of the present paper. Indeed, it is difficult to capture at reaction temperature the structure of materials that stick to the plates. Moreover, the structure can be affected by cooling.

The rheological behavior, combined with mass loss, is a very significant "signature" of thermal degradation of materials. We noticed different rheological signatures for different lignins (not shown) that would depend on initial lignin structure (cross-linking, molecular weight, functional groups, heteroatoms). Further investigations are needed to understand the relations between rheological behavior, volatiles products, and lignin composition.

Concerning cellulose, the evolutions of the viscous and elastic moduli are very different from those for lignin (Figure 5b). The material stays roughly hard (high moduli) through the degradation, but both moduli decrease sharply at about 320 °C, before the temperature of maximum mass loss. A mild softening is thus evidenced even for this slow heating rate (5 K min⁻¹), consistent with the formation of mobile protons. Cellulose would even form a material with high viscous contribution during a short temperature range close to maximum mass loss temperature (335 °C). Undoubtedly, a viscoelastic liquid could be formed at higher heating rates.^{28–30}

Concerning xylan, softening starts at 220 °C after the beginning of mass loss and solidification at 270 °C at about 75% mass loss (on anhydrous basis, Figure 5c). It can be noticed that solidification is very fast, just as for lignin, and lead to a very elastic and hard char less fluffy and much harder than the lignin char.

Miscanthus (Figure 5d) exhibits very different viscoelastic properties than the other three materials. The contribution of xylan and cellulose can be seen at 270 and 330 °C, respectively, but lignin softening is not seen.

The elastic moduli of the four materials are compared in Figure 7. The elastic modulus of extracted lignin is 3 orders of

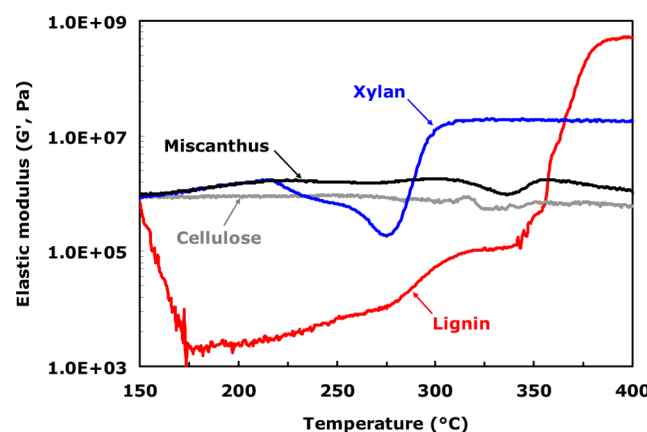


Figure 7. Comparison of elastic modulus evolution as a function of temperature for lignin, cellulose, xylan, and Miscanthus. The variation of elastic modulus for lignin is 3 orders of magnitude higher than that for Miscanthus. Nevertheless, lignin has no apparent contribution on the viscoelastic behavior of Miscanthus.

magnitude lower than that for Miscanthus during softening and 3 orders of magnitude higher after solidification. However, the contribution of lignin to the rheological signature of Miscanthus is not captured. This finding is again in agreement with ^1H NMR analysis and with ref 16. In the native network of biomass, lignin is linked to xylan and xylan to cellulose.⁵⁸ The rigidity of lignin fragments could be maintained by xylan before its thermal degradation and indirectly by cellulose. The elastic moduli of Miscanthus and cellulose have similar patterns on the logarithmic scale used in Figure 7. Cellulose imposes its

viscoelastic behavior to the overall degraded polymer network from the native Miscanthus. Further work is needed to better understand the effect of the native cellulose composition on biomass char structure.

$\tan(\delta)$ (see eq 4) is an important parameter to compare the viscoelastic behavior of materials. Indeed, a material can be soft (low elastic modulus), but if the elastic modulus is higher than the viscous modulus, it could be soft but mainly elastic.

Lignin produces a material that is mainly elastic from 200 °C (Figure 8), even if it is soft from 150 to 350 °C (low elastic

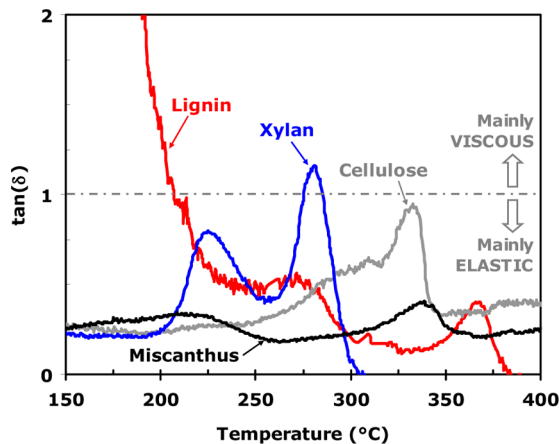
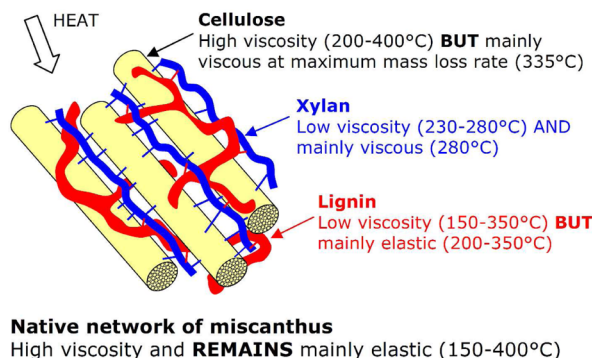


Figure 8. Evolution of $\tan(\delta)$ as a function of temperature.

modulus). On the contrary, cellulose gives rise to a hard material through pyrolysis that becomes almost viscous at 335 °C (under our heating conditions). Xylan pyrolysis produces a soft and mainly viscous intermediate material at 270 °C. Miscanthus remains mainly elastic even if cellulose becomes almost mainly viscous at 335 °C. All these findings are summed-up in Scheme 2.

Scheme 2. Simplified Scheme of Polymers Network in Native Biomass. The Main Findings from in Situ Rheology Analysis for the Fractionated Polymers and the Native Biomass Are Summed Up



3.3. Swelling and Shrinking Behaviors Obtained by in Situ Measurement of Rheometer Plates' Axial Displacement. The vertical displacement (ΔL) between the plates of the rheometer was also measured during pyrolysis. It gives in situ the swelling and shrinking behaviors of the materials in real-time and -temperature.

Vertical displacement (ΔL) has been normalized by the initial thickness (~ 2 mm for all materials) and is presented in Figure 9.

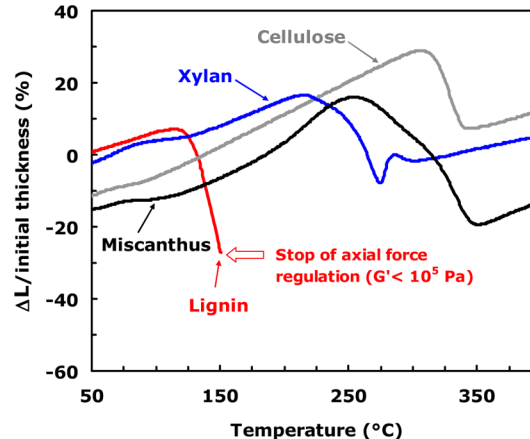


Figure 9. Evolution of displacement between plates (ΔL) as a function of temperature revealing thermal dilatation of materials (and rheometer), swelling, and shrinking behaviors of materials undergoing pyrolysis (5 K min^{-1}) in real-time and -temperature.

Parts of the curve with a linear evolution of ΔL as a function of temperature (low temperature for cellulose, high temperature after char solidification, Figure 9) are attributed to thermal dilatation of the rheometer and biomass/char.

A nonlinear thermal expansion of Miscanthus is evidenced between 150 and 250 °C, followed by a shrinking related to mass loss (Figure 5d). Shrinking of cellulose and xylan also starts with mass loss at 310 and 220 °C, respectively. Apparent shrinking of lignin is due to its softening from 130 °C and the normal force imposed by the upper plate (200 g). Normal force regulation is stopped at 150 °C for lignin, and the plates' displacement becomes meaningless. We noticed different swelling behaviors of lignins (not shown). Other lignins can generate a higher flow rate of volatiles within a less soft material (higher G'). Accordingly, the volatiles were able to "push" the intermediate viscoelastic material, thus maintaining the axial force autoregulation.

Wada and co-workers^{59,60} studied the thermal expansion of cellulose by in situ X-ray diffraction under the same heating rate than ours (5 K min^{-1}). It was suggested that the anisotropic thermal expansion of wood is mainly caused by the morphology and structure of cellulose in wood.⁵⁹ It is consistent with our ^1H NMR and rheology analysis, showing that cellulose tends to "impose" its behavior to the polymer network during pyrolysis. Cellulose forms another "high temperature" crystalline phase resulting in an anisotropic thermal expansion.^{59,60} In our case, crystals of cellulose (in microgranular cellulose and in Miscanthus) are randomly oriented in the biomass disk due to the high number of particles. Consequently, only an overall expansion can be measured along the vertical axes.

The expansion of Miscanthus until 250 °C is in agreement with the work of Haas et al.,²⁰ who quantified in situ the expansion by microscope imaging. They explained the expansion by a "heat-induced expansion of the gaseous contents of the biomass, expansion, or phase change of specific molecular species in the cell wall, such as lignin, or release of gases from chemical reactions taking place".²⁰

It is known that the ultrastructure of biomass cell wall can be related to the solubility parameters of polymers.⁶¹ Moreover, cellulose is deformable under the action of sorption forces that leads to swelling.⁶² Xylan was shown to form mobile compounds from 225 °C, and lignin is completely mobile from 200 °C (Figure 4). The mobile species formed by lignin and xylan thermal conversion could cause a swelling of biomass cell walls. Cellulose chains would maintain the overall coherence of cell walls^{31,58} and could be swelled by soluble intermediate mobile species.

To summarize, the thermal expansion of Miscanthus is higher than microgranular cellulose possibly due to (i) a different structure of cellulose in Miscanthus that leads to different expansion of cellulose crystallites and (ii) a swelling effect on cellulose of mobile intermediate products (probably mainly xylan mobile products).

After swelling, contraction is discussed. The contraction phase for Miscanthus starts at 250 °C, at a lower temperature than in Haas et al.²⁰ (above 350 °C), probably due to different heat and mass transfer conditions, biomass composition, and analytical method to investigate contraction. They observed during contraction that the remaining solid cell wall material collapses the cell lumen as some of the liquid-phase material flows out of the cell wall and explained contraction by two phenomena: (i) liquid and gas-phase products leaving the biomass, taking up less volume, and (ii) weakened cell walls and tears and cracks allow the largest cell lumina.²⁰

Finally, after the contraction of xylan a fast swelling is evidenced from 275 to 285 °C (Figure 9) at the beginning of the solidification stage (275–300 °C). It coincides with the maximum mass loss rate (275 °C) producing a high flow rate of volatiles that pushes the viscoelastic material.

3.4. Relations between ¹H NMR and Rheology Analysis. Figure 10 displays the elastic modulus as a function of fluid phase fraction. The physical analysis from rheology is thus compared to the chemical analysis from ¹H NMR.

It has been previously shown that the rheological properties of coal and some blends could be related with the mobile protons.⁴² Biomass and its constituents have a completely different pattern than coal because of the different origin in mobility formation between biomass constituents and coal.

Figure 10a shows an almost linear relationship during softening of xylan and lignin, but when solidification proceeds, mobile protons remain in the elastic solid-like char. This finding is in agreement with Haas et al.,²⁰ who show that pyrolysis products are entrapped in heat-treated wood. To the best of our knowledge, we provide the first quantification of formed and entrapped mobile products in real-time and temperature.

It is evidenced that molecular mobility is formed during cellulose pyrolysis in a mainly elastic material with few variations in elastic modulus compared with mobile protons (Figure 10b). This finding is in agreement and supports the concept of "cavities" extensively developed by Mamleev et al.³⁰ High-boiling liquid tar are encapsulated in the cavities (nuclei) and launch the ionic mechanisms occurring in cellulose pyrolysis.³⁰

Furthermore, the materials can present dispersions or suspensions. The liquid phase can fill up an interfibrillar space and coat solid particles.⁵⁵ Further research works are needed to better understand the scale and nature of interactions between the liquid phase and solid materials.

Regarding Miscanthus, it can be seen from Figure 10b that native biomass leads to a much more complex behavior than

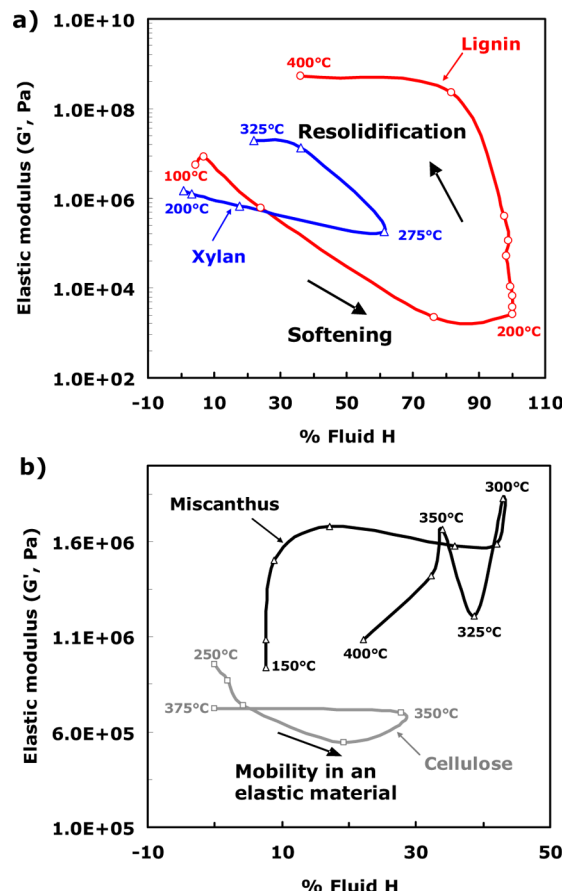


Figure 10. Evolution of elastic modulus (G' , from rheology analysis) as a function of mobile protons (% fluid H, from ^{1}H NMR analysis) for (a) xylan and lignin and (b) cellulose and Miscanthus. Mobility (% fluid H) is still present after solidification of lignin and xylan. Mobility of cellulose occurs in an elastic material, in solid-like cavities.

separated polymers. Further investigations are needed with other complementary methods such as ^{13}C NMR⁶³ to better understand the intermediate materials formed in the network of polymers/char.

4. CONCLUSION

To the best of our knowledge, we provide the first *in situ* ^{1}H NMR and rheology analysis for the pyrolysis of biomass (*Miscanthus x Giganteus*), microgranular cellulose, xylan, and ethanol organosolv lignin extracted from Miscanthus. These methods have been used for coal pyrolysis for a long time but not yet for biomass polymers. The extent of softening is measured by these two complementary methods in real-time and -temperature conditions. ^{1}H NMR gives the fraction of mobile protons and rheology the viscoelastic behaviors (elastic and viscous moduli).

From rheology measurements, we showed that the extracted lignin produces a material that is mainly elastic from 200 °C, even if it is a soft material from 150 to 350 °C (low elastic modulus). On the contrary, cellulose gives rise to a hard material through pyrolysis, which becomes almost viscous at 335 °C (under our heating conditions). Xylan pyrolysis produces a soft and mainly viscous intermediate material at 270 °C. Miscanthus remains mainly elastic. Cellulose tends to "impose" its visco-elastic behavior in the native polymer

network of Miscanthus. The mechanisms of softening, swelling, shrinking, and char formation are discussed.

Rheology results are compared to ^1H NMR data. It is shown that mobility is formed in a mainly elastic material during cellulose and Miscanthus pyrolysis supporting the concept of "cavities" in which liquid tar are encapsulated.

Further works are still needed to better understand these phenomena by means of other techniques such as ^{13}C NMR and imaging. This work needs also to be extended to higher heating rates.

Many works have dealt with biomass pyrolysis. We have reported studies on biomass pyrolysis for the beginning of the 19th century.⁶⁴ Some past studies in biomass pyrolysis have been "forgotten" and may need to be reappropriated. Nevertheless, the knowledge in biomass pyrolysis seems to be less advanced than for coal or synthetic polymers degradation. Further works on non-intrusive *in situ* analysis could give new insights into the fundamentals of biomass pyrolysis, which are yet needed to better design reactors and future biorefineries.

AUTHOR INFORMATION

Corresponding Author

*Phone: +33 3 83 17 50 78. E-mail: anthony.dufour@ensic.inpl-nancy.fr.

Notes

The authors declare no competing financial interest.

ACKNOWLEDGMENTS

S. Hoppe and V. Falk (Lorraine University-CNRS) are kindly acknowledged for providing some equipment. The research leading to these results has received funding from the European Union's Research Programme of the Research Fund for Coal and Steel (RFCS) research programme under Grant Agreement No. [RFCR-CT-2010-00007], the French National Research Agency (ANR, PYRAIM project), and the Energy Program of CNRS (CRAKIN project).

REFERENCES

- (1) Villermaux, J.; Antoine, B.; Lede, J.; Soulignac, F. *Chem. Eng. Sci.* **1986**, *41*, 151–157.
- (2) Lédé, J. *Energies* **2010**, *3*, 886–898.
- (3) Gaston, K. R.; Jarvis, M. W.; Pepiot, P.; Smith, K. M.; Frederick, W. J.; Nimlos, M. R. *Energy Fuels* **2011**, *25*, 3747–3757.
- (4) Shen, J.; Wang, X.-S.; Garcia-Perez, M.; Mourant, D.; Rhodes, M. J.; Li, C.-Z. *Fuel* **2009**, *88*, 1810–1817.
- (5) Dufour, A.; Girods, P.; Masson, E.; Rogaume, Y.; Zoulalian, A. *Int. J. Hydrogen Energy* **2009**, *34*, 1726–1734.
- (6) Mok, W. S.-L.; Antal, M. J., Jr. *Thermochim. Acta* **1983**, *68*, 165–186.
- (7) Broido, A.; Javier-Son, A. C.; Ouano, A. C.; Barrall, E. M. *J. Appl. Polym. Sci.* **1973**, *17*, 3627–3635.
- (8) Shafizadeh, F. *J. Anal. Appl. Pyrolysis* **1982**, *3*, 283–305.
- (9) Evans, R. J.; Milne, T. A. *Energy Fuels* **1987**, *1*, 123–137.
- (10) Faix, O.; Fortmann, I.; Bremer, J.; Meier, D. *Holz Roh- Werkst.* **1991**, *49*, 299–304.
- (11) Wooten, J. B.; Seeman, J. I.; Hajaligol, M. R. *Energy Fuels* **2004**, *18*, 1–15.
- (12) Stoeckli, H. F. *Carbon* **1990**, *28*, 1–6.
- (13) Kollmann, F. F. P.; Sachs, I. B. *Wood Sci. Technol.* **1967**, *1*, 14–25.
- (14) McGinnes, E. A.; Kandeel, S. A.; Szopa, P. S. *Wood Fiber* **1971**, *3*, 77–83.
- (15) Fisher, T.; Hajaligol, M.; Waymack, B.; Kellogg, D. *J. Anal. Appl. Pyrolysis* **2002**, *62*, 331–349.
- (16) Baliga, V.; Sharma, R.; Miser, D.; McGrath, T.; Hajaligol, M. *J. Anal. Appl. Pyrolysis* **2003**, *66*, 191–215.
- (17) Sharma, R. K.; Wooten, J. B.; Baliga, V. L.; Lin, X.; Chan, W. G.; Hajaligol, M. R. *Fuel* **2004**, *83*, 1469–1482.
- (18) Boonstra, M. J.; Rijsdijk, J. F.; Sander, C.; Kegel, E.; Tjeerdsma, B.; Militz, H.; Van Acker, J.; Stevens, M. *Maderas: Ciencia y Tecnología* **2006**, *8*, 193–208.
- (19) Biagini, E.; Narducci, P.; Tognotti, L. *Fuel* **2008**, *87*, 177–186.
- (20) Haas, T. J.; Nimlos, M. R.; Donohoe, B. S. *Energy Fuels* **2009**, *23*, 3810–3817.
- (21) Jarvis, M. W.; Haas, T. J.; Donohoe, B. S.; Daily, J. W.; Gaston, K. R.; Frederick, W. J.; Nimlos, M. R. *Energy Fuels* **2011**, *25*, 324–336.
- (22) Kwon, S.-M.; Kim, N.-H.; Cha, D.-S. *Wood Sci. Technol.* **2009**, *43*, 487–498.
- (23) Welzbacher, C. R.; Rassam, G.; Talaei, A.; Brischke, C. *Wood Mater. Sci. Eng.* **2011**, *6*, 219–227.
- (24) Dufour, A.; Ouartassi, B.; Bounaceur, R.; Zoulalian, A. *Chem. Eng. Res. Des.* **2011**, *89*, 2136–2146.
- (25) Axelson, D. E.; Wooten, J. B. *J. Anal. Appl. Pyrolysis* **2007**, *78*, 214–227.
- (26) Goring, D. A. I. *Pulp Pap. Mag. Can.* **1963**, *64*, 517–527.
- (27) Nordin, S. B.; Nyren, J. O.; Back, E. L. *Textile Res.* **1974**, *44*, 152–154.
- (28) Boutin, O.; Ferrer, M.; Lédé, J. *J. Anal. Appl. Pyrolysis* **1998**, *47*, 13–31.
- (29) Piskorz, J.; Majerski, P.; Radlein, D.; Vladars-Usas, A.; Scott, D. S. *J. Anal. Appl. Pyrolysis* **2000**, *56*, 145–166.
- (30) Mamleev, V.; Bourbigot, S.; Le Bras, M.; Yvon, J. *J. Anal. Appl. Pyrolysis* **2009**, *84*, 1–17.
- (31) Dufour, A.; Castro-Díaz, M.; Brosse, N.; Bouroukba, M.; Snape, C. *ChemSusChem* **2012**, *5*, 1258–1265.
- (32) Klason, P.; Heidenstrom, G. V.; Norlin, E. Z. *Angew. Chem.* **1910**, *23*, 1252–1257.
- (33) Lédé, J.; Li, H. Z.; Villermaux, J.; Martin, H. *J. Anal. Appl. Pyrolysis* **1987**, *10*, 291–308.
- (34) Narayan, R.; Antal, M. J., Jr. *Ind. Eng. Chem. Res.* **1996**, *35*, 1711–1721.
- (35) Miyazawa, K.; Yokono, T.; Sanada, Y. *Carbon* **1979**, *17*, 223–225.
- (36) Sakurovs, R.; Lynch, L. J.; Maher, T. P.; Banerjee, R. N. *Energy Fuels* **1987**, *1*, 167–172.
- (37) Yoshida, T.; Takanohashi, T.; Iino, M.; Kumagai, H.; Kato, K. *Energy Fuels* **2004**, *18*, 349–356.
- (38) Maroto-Valer, M. M.; Andréseen, J. M.; Snape, C. E. *Energy Fuels* **1997**, *11*, 236–244.
- (39) Xiong, J.; Maciel, G. E. *Energy Fuels* **1997**, *11*, 856–865.
- (40) Sakurovs, R. *Fuel* **2003**, *82*, 1911–1916.
- (41) Díaz, M. C.; Steel, K. M.; Drage, T. C.; Patrick, J. W.; Snape, C. E. *Energy Fuels* **2005**, *19*, 2423–2431.
- (42) Díaz, M. C.; Edecki, L.; Steel, K. M.; Patrick, J. W.; Snape, C. E. *Energy Fuels* **2008**, *22*, 471–479.
- (43) Castro-Díaz, M.; Zhao, H.; Kokonya, S.; Dufour, A.; Snape, C. E. *Energy Fuels* **2012**, *26*, 1767–1775.
- (44) Diez, M. A.; Alvarez, R.; Fernández, M. *Fuel* **2012**, *96*, 306–313.
- (45) El Hage, R.; Brosse, N.; Sannigrahi, P.; Ragauskas, A. *Polym. Degrad. Stab.* **2010**, *95*, 997–1003.
- (46) Parks, T. J.; Cross, L. F.; Lynch, L. J. *Carbon* **1991**, *29*, 921–927.
- (47) Sakurovs, R.; Lynch, L. J. *Fuel* **1993**, *72*, 743–749.
- (48) Steel, K. M.; Diaz, M. C.; Patrick, J. W.; Snape, C. E. *Energy Fuels* **2004**, *18*, 1250–1256.
- (49) Jakab, E.; Faix, O.; Till, F.; Székely, T. *J. Anal. Appl. Pyrolysis* **1995**, *35*, 167–179.
- (50) Nakamura, T.; Kawamoto, H.; Saka, S. *J. Anal. Appl. Pyrolysis* **2008**, *81*, 173–182.
- (51) Brosse, N.; El Hage, R.; Chaouch, M.; Pétrissans, M.; Dumarcay, S.; Gérardin, P. *Polym. Degrad. Stab.* **2010**, *95*, 1721–1726.
- (52) Faravelli, T.; Frassoldati, A.; Migliavacca, G.; Ranzi, E. *Biomass Bioenergy* **2010**, *34*, 290–301.
- (53) Wang, N.; Low, M. J. D. *Mater. Chem. Phys.* **1990**, *26*, 67–80.

- (54) Suuberg, E. M.; Milosavljevic, I. O. V. *Proc. Int. Symp. Combust.* **1996**, *26*, 1515–1521.
- (55) Donohoe, B. S.; Decker, S. R.; Tucker, M. P.; Himmel, M. E.; Vinzant, T. B. *BioTechnol. Bioeng.* **2008**, *101*, 913–925.
- (56) Zakzeski, J.; Bruijnincx, P. C. A.; Jongerius, A. L.; Weckhuysen, B. M. *Chem. Rev.* **2010**, *110*, 3552–3599.
- (57) Newman, R. H. *Holzforschung* **1992**, *46*, 205–210.
- (58) Jarvis, M. C.; McCann, M. C. *Plant Physiol. Biochem.* **2000**, *38*, 1–13.
- (59) Hori, R.; Wada, M. *Cellulose* **2005**, *12*, 479–484.
- (60) Wada, M.; Hori, R.; Kim, U.-J.; Sasaki, S. *Polym. Degrad. Stab.* **2010**, *95*, 1330–1334.
- (61) Hansen, C. M.; Björkman, A. *Holzforschung* **1998**, *52*, 335–344.
- (62) Chirkova, J.; Andersson, B.; Andersone, I. *BioResources* **2009**, *4*, 1044–1057.
- (63) Le Brech, Y.; Castro-Diaz, M.; Snape, C. E.; Brosse, N.; Delmotte, L.; Bouroukba, M.; Marchal, P.; Dufour, A. Investigation of biomass pyrolysis by in-situ ¹H NMR, rheology and ex-situ ¹³C NMR. *19th International Symposium on Analytical and Applied Pyrolysis*, Linz, Austria, May 2012.
- (64) Mollerat, J. B. *Mémoires Présentés À L'Institut Sur La Distillation Du Bois Et L'Emploi De Ses Produits*; Bernard, V., Ed.; Bibliothèque National de France: Paris, **1808**; p 58.